Discovery of novel steroidal pyran-oxindole hybrids as cytotoxic agents

ARTICLE *in* STEROIDS · OCTOBER 2014

Impact Factor: 2.64 · DOI: 10.1016/j.steroids.2014.05.022

6 AUTHORS, INCLUDING:

BIN YU
Zhengzhou University
34 PUBLICATIONS **279** CITATIONS
SEE PROFILE

Ping-ping Qi
Zhengzhou University
11 PUBLICATIONS **40** CITATIONS
SEE PROFILE

Li-Hong Shan
Zhengzhou University
8 PUBLICATIONS **35** CITATIONS
SEE PROFILE

Hong-Min Liu
Zhengzhou University
174 PUBLICATIONS **1,408** CITATIONS
SEE PROFILE

Steroids 88 (2014) 44–52

Contents lists available at ScienceDirect

Steroids

journal homepage: www.elsevier.com/locate/steroids

Discovery of novel steroidal pyran–oxindole hybrids as cytotoxic agents

Bin Yu [1], Ping-Ping Qi [1], Xiao-Jing Shi, Li-Hong Shan *, De-Quan Yu *, Hong-Min Liu *

School of Pharmaceutical Sciences and New Drug Research & Development Center, Zhengzhou University, Zhengzhou 450001, PR China

ARTICLE INFO

Article history:
Received 18 March 2014
Received in revised form 14 May 2014
Accepted 25 May 2014
Available online 11 June 2014

Keywords:
Pyran–oxindole hybrids
Cytotoxicity
Apoptosis
Cell cycle arrest

ABSTRACT

A series of novel steroidal pyran–oxindole hybrids were efficiently synthesized in a single operation through the vinylogous aldol reaction of vinyl malononitrile **3** with substituted isatins involving the construction of C–C and C–O bonds. Some compounds displayed moderate to good cytotoxicity against T24, SMMC-7721, MCF-7 and MGC-803 cells. Compounds **4f** and **4i** were more potent than 5-Fu against T24 and MGC-803 cells with the IC_{50} values of 4.43 and 8.45 μM, respectively. Further mechanism studies indicated that compound **4i** induced G2/M arrest and early apoptosis in a concentration- and time-dependent manner.

1. Introduction

Steroids are extensively available in nature and well known for their profound biological activities due to their high ability to penetrate cells and bind to nuclear and membrane receptors. Chemical modifications of the steroid ring system and side chain provide a way to alter the functional groups and numerous structure–activity relationships have been established by such synthetic alterations [1,2]. It is proved that a number of biologically important properties of modified steroids are dependent upon structural features of the steroid ring system and side chain [3–6]. In recent years, a number of steroidal heterocycles with interesting activities have been isolated or synthesized. For example, spironolactone, as the mineralocorticoid antagonist, is a clinically used drug for congestive heart failure (Fig. 1) [7]. A recent report from Puranik Purushottamachar *et al.* described that galeterone analogue had potential for development as new drugs for the treatment of all forms of prostate cancer with an IC_{50} value of 0.87 μM through degrading both full-length and truncated ARs in CWR22rv1 human prostate cancer cells [8]. Our group recently reported that [1,2,4] triazolo [1,5-a] pyrimidine-based phenyl-linked steroid dimer induced apoptosis through the mitochondrial pathway accompanied with the decrease of mitochondrial membrane potential, activations of caspase-9/-3, cleavage of MDM2 as well as upregulation of the expressions of p53 and Bax [9].

The oxindole nucleus is a privileged scaffold that is highly prevalent in natural and synthetic compounds of medicinal interest [10]. Molecules containing an oxindole nucleus display a diverse range of biological activities [11], such as inhibitors of the MDM2-p53 interaction [12], antimicrobial activities [13], cholinesterase inhibitors [14,15], anticancer properties [16], protein kinase activators [17] and so on. Particularly intriguing is the NITD609, which has been studied as an antimalarial drug candidate that acts through the distinct mechanism of action as existing antimalarial drugs have [18]. Besides, oxindoles can also serve as synthetic intermediates for alkaloids and many kinds of pharmaceuticals or drug precursors [19]. Fox example, coerulescine, the simplest spirooxindole–pyrrolidine hybrid found in nature, displays local anesthetic effect [10]. The spirotryprostatins have antimitotic properties and are of interest as anticancer lead compounds [20], and the recently discovered small-molecule MDM2 inhibitor MI-219 and its analogues are in preclinical development for cancer therapeutics (Fig. 2) [12,21]. Additionally, the six-membered pyran ring system, as an important structural motif, is also found in a wide range of biologically active compounds and is known to have wide applications in medicinal chemistry [22]. For example, pyrrolo [2, 3-h] chromenes (Fig. 2) showed excellent anticancer activity with an EC_{50} value of 13 nM against T47D cells [23,24].

On the basis of the above-mentioned observations regarding the potential of oxindoles and pyrans and our own previous observations regarding [25] the importance of the steroidal oxindoles in conferring cytotoxic activities, a series of steroidal pyran–oxindole hybrids were designed, incorporating both oxindole and

* Corresponding authors. Tel./fax: +86 371 67781739.
E-mail addresses: zzuyubin@hotmail.com (B. Yu), shlh@zzu.edu.cn (L.-H. Shan), dqyu@imm.ac.cn (D.-Q. Yu), liuhm@zzu.edu.cn (H.-M. Liu).
[1] These authors made equal contributions.

http://dx.doi.org/10.1016/j.steroids.2014.05.022
0039-128X/

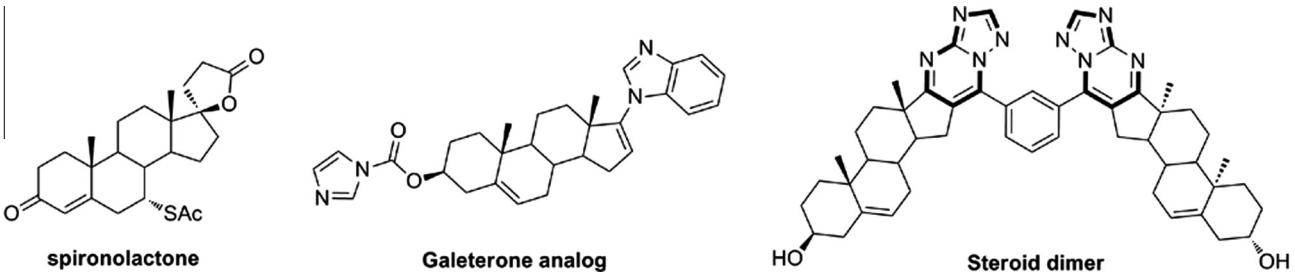

Fig. 1. Selective biologically active steroidal compounds.

2-imino-3-cyano pyran key scaffolds, with an aim to obtain potent and selective cytotoxic agents. Besides, we also explored the effects toward the cell cycle and possible mechanism of inducing apoptosis.

2. Experimental section

2.1. General

Reagents and solvents were purchased from commercial sources and were used without further purification. Isatins used were purchased from Aladdin Company (www.aladdin-e.com). Thin-layer chromatography (TLC) was carried out on glass plates coated with silica gel (Qingdao Haiyang Chemical Co., G60F-254) and visualized by UV light (254 nm). The products were purified by column chromatography over silica gel (Qingdao Haiyang Chemical Co., 200-300 mesh). Melting points were determined on a X-5 micromelting apparatus and are uncorrected. All the NMR spectra were recorded with a Bruker DPX 400 MHz spectrometer with TMS as internal standard in $CDCl_3$. Chemical shifts are given as δ ppm values relative to TMS (Most of the peaks due to the steroidal skeleton are merged and could not be differentiated. Thus δ values of only those peaks that distinguish the product and could easily be differentiated are reported). High-resolution mass spectra (HRMS) were recorded on a Waters Micromass Q-T of Micromass spectrometer by electrospray ionization (ESI).

2.2. Synthesis of steroidal α, α-dicyanoalkene (**3**)

The steroidal α, α-dicyanoalkene (**3**) was efficiently prepared via Aldol condensation of 3β-acetyl dehydroepiandrosterone **2** with malononitrile in ethanol catalyzed by ammonium acetate according to our previously reported method [4,6].

2.3. General procedure for the synthesis of steroidal pyran–oxindole hybrids ***4a–j***

To a solution of compound **3** (1.0 mmol) and substituted isatin (1.0 mmol) in ethanol, 1, 8-diazabicyclo [5.4.0] undec-7-ene (DBU) (2.0 mmol) was added. The reaction mixture was stirred at room temperature for about 1 h. The solvent was removed and CH_2Cl_2 was added, the organic phase was washed with water and brine, dried over Na_2SO_4. After removal of the solvent, the residue was purified by silica gel chromatography using acetone/petroleum ether (1/2) as the eluent to give the corresponding steroidal pyran–oxindole hybrids.

2.3.1. Compound ***4a***

White solid, yield: 75%, m. p. 230.7–232.0 °C. ^{1}H NMR (400 MHz, $CDCl_3$) δ 9.41 (s, 1H), 7.18 (d, *J* = 8.2 Hz, 1H), 7.10 (d, *J* = 7.9 Hz, 1H), 7.06 (d, *J* = 5.5 Hz, 1H), 6.56 (d, *J* = 7.6 Hz, 1H), 5.29 (s, 1H), 4.69–4.51 (m, 1H), 3.96 (s, 1H), 2.04 (s, 3H), 1.56 (s, 3H), 1.06 (s, 3H). ^{13}C NMR (100 MHz, $CDCl_3$) δ 191.66, 175.50, 170.57, 169.41, 143.96, 139.93, 131.45, 127.39, 124.40, 121.25, 119.99, 112.20, 110.23, 104.38, 73.49, 72.66, 57.16, 56.05, 49.28, 47.70, 37.97, 36.74, 36.64, 34.60, 32.27, 30.45, 29.28, 27.60, 21.40, 19.98, 19.29, 15.57. HRMS (ESI): *m/z* calcd for $C_{32}H_{34}BrN_3NaO_4$ $(M + Na)^+$, 626.1630; found, 626.1654.

2.3.2. Compound ***4b***

Yellow solid, yield: 78%, m. p. 232.1–233.7 °C. ^{1}H NMR (400 MHz, $CDCl_3$) δ 9.51 (s, 1H), 7.19 (s, 1H), 7.18–7.10 (m, 1H),

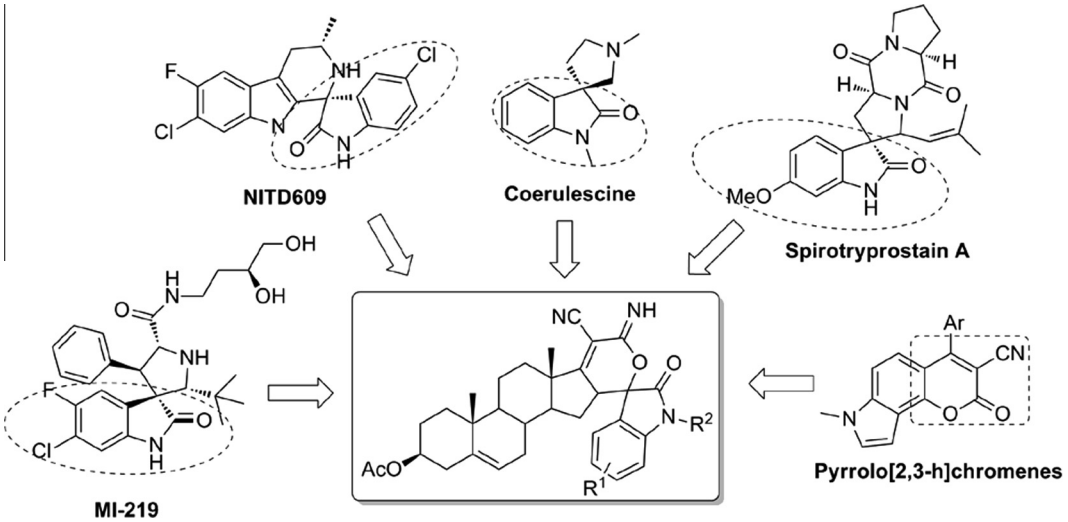

Fig. 2. Designed strategy of steroidal pyran–oxindole hybrids. The dashed boxes indicate the key core structure present in previously reported molecules.

7.01 (d, J = 7.8 Hz, 1H), 6.47 (d, J = 7.2 Hz, 1H), 5.30 (s, 1H), 4.61 (s, 1H), 4.03 (d, J = 6.3 Hz, 1H), 2.04 (s, 3H), 1.53 (s, 3H), 1.06 (s, 3H). ^{13}C NMR (100 MHz, $CDCl_3$) δ 191.50, 175.58, 170.54, 169.29, 143.79, 139.94, 131.27, 131.23, 124.34, 121.97, 121.27, 112.05, 109.57, 103.66, 73.50, 72.63, 57.24, 55.12, 49.35, 47.43, 37.98, 36.75, 36.64, 34.52, 32.45, 32.26, 30.44, 27.61, 21.40, 20.01, 19.31, 15.14. HRMS (ESI): m/z calcd for $C_{32}H_{35}ClN_3O_4$ $(M + H)^+$, 560.2316; found, 560.2316.

2.3.3. Compound **4c**

White solid, yield: 83%, m. p. 254.3–255.6 °C. ^{1}H NMR (400 MHz, $CDCl_3$) δ 7.27 (m, 6H), 7.01 (t, J = 7.6 Hz, 1H), 6.92 (d, J = 7.4 Hz, 1H), 6.73 (d, J = 7.9 Hz, 1H), 6.21 (s, 1H), 5.39 (s, 1H), 5.14 (d, J = 15.7 Hz, 1H), 4.72–4.52 (m, 2H), 4.05 (s, 1H), 2.04 (s, 3H), 1.46 (s, 3H), 1.09 (s, 3H). ^{13}C NMR (100 MHz, $CDCl_3$) δ 189.05, 174.28, 170.48, 167.96, 143.73, 139.85, 135.44, 129.69, 129.00, 127.92, 127.29, 125.86, 122.51, 122.13, 121.43, 111.87, 109.81, 104.42, 73.53, 71.10, 57.54, 55.37, 49.62, 45.86, 44.08, 37.99, 36.79, 36.66, 34.36, 33.68, 32.45, 30.27, 27.63, 21.40, 20.08, 19.36, 14.68. HRMS (ESI): m/z calcd for $C_{39}H_{41}N_3NaO_4$ $(M + Na)^+$, 638.2995; found, 638.2994.

2.3.4. Compound **4d**

White solid, yield: 80%, m. p. 245.4–247.6 °C. ^{1}H NMR (400 MHz, $CDCl_3$) δ 7.18 (t, J = 7.6 Hz, 3H), 7.08 (d, J = 4.6 Hz, 1H), 7.00 (td, J = 7.3, 2.6 Hz, 1H), 6.94 (d, J = 7.3 Hz, 1H), 6.92–6.85 (m, 1H), 6.58–6.42 (m, 1H), 5.37 (d, J = 3.6 Hz, 1H), 5.14 (dd, J = 16.6, 8.1 Hz, 1H), 4.68–4.54 (m, 1H), 4.55–4.33 (m, 1H), 4.08 (s, 1H), 2.40 (s, 3H), 2.04 (s, 3H), 1.47 (s, 3H), 1.09 (s, 3H). ^{13}C NMR (100 MHz, $CDCl_3$) δ 189.27, 174.18, 170.49, 144.10, 139.82, 135.68, 132.98, 130.67, 129.63, 127.51, 126.31, 125.75, 122.19, 121.47, 111.93, 110.04, 104.38, 100.00, 73.54, 57.66, 55.31, 49.63, 45.85, 42.13, 37.99, 36.78, 36.66, 34.39, 33.59, 32.44, 30.26, 27.63, 21.41, 20.08, 19.37, 14.67. HRMS (ESI): m/z calcd for $C_{40}H_{44}N_3O_4$ $(M + H)^+$, 630.3332; found, 630.3329.

2.3.5. Compound **4e**

White solid, yield: 79%, m. p. 236.7–239.0 °C. ^{1}H NMR (400 MHz, $CDCl_3$) δ 7.23–7.17 (m, 2H), 7.07 (t, J = 6.4 Hz, 3H), 7.00 (d, J = 7.5 Hz, 1H), 6.92 (d, J = 7.4 Hz, 1H), 6.75 (d, J = 8.1 Hz, 1H), 6.18 (s, 1H), 5.38 (d, J = 3.4 Hz, 1H), 5.10 (d, J = 15.7 Hz, 1H), 4.63 (m, 1H), 4.57 (d, J = 15.7 Hz, 1H), 4.05 (s, 1H), 2.31 (s, 3H), 2.04 (s, 3H), 1.46 (s, 3H), 1.09 (s, 3H). ^{13}C NMR (100 MHz, $CDCl_3$) δ 189.06, 174.29, 170.49, 167.97, 143.83, 139.85, 138.81, 135.39, 129.69, 128.85, 128.69, 127.89, 124.34, 122.45, 122.14, 121.44, 111.90, 109.84, 104.41, 73.53, 71.13, 57.54, 55.36, 49.63, 45.84, 44.05, 37.99, 36.78, 36.72, 36.66, 34.36, 33.67, 32.44, 30.27, 27.63, 21.41, 20.07, 19.36, 14.69. HRMS (ESI): m/z calcd for $C_{40}H_{44}N_3O_4$ $(M + H)^+$, 630.3332; found, 630.3331.

2.3.6. Compound **4f**

White solid, yield: 80%, m. p. 218.1–220.5 °C. ^{1}H NMR (400 MHz, $CDCl_3$) δ 7.22 (d, J = 7.4 Hz, 1H), 7.20–7.14 (m, 2H), 7.11 (d, J = 7.9 Hz, 2H), 6.97 (d, J = 7.3 Hz, 1H), 6.90 (d, J = 7.4 Hz, 1H), 6.76 (d, J = 7.9 Hz, 1H), 6.60 (s, 1H), 5.37 (d, J = 4.9 Hz, 1H), 5.14 (d, J = 16.0 Hz, 1H), 4.61 (dd, J = 16.0, 9.8 Hz, 2H), 4.04 (s, 1H), 2.30 (s, 3H), 2.04 (s, 3H), 1.45 (s, 3H), 1.09 (s, 3H). ^{13}C NMR (100 MHz, $CDCl_3$) δ 189.21, 174.27, 170.50, 168.28, 143.84, 139.81, 137.57, 132.53, 129.60, 129.42, 127.45, 127.32, 125.74, 122.38, 122.15, 121.47, 111.92, 109.86, 104.38, 93.86, 73.54, 71.30, 57.57, 55.30, 49.62, 45.82, 43.93, 37.98, 36.79, 36.65, 36.50, 34.35, 33.59, 32.44, 30.23, 27.63, 21.41, 21.10, 19.36, 14.66. HRMS (ESI): m/z calcd for $C_{40}H_{44}N_3O_4$ $(M + H)^+$, 630.3332; found, 630.3329.

2.3.7. Compound **4g**

White solid, yield: 84%, m. p. 242.5–247.6 °C. ^{1}H NMR (400 MHz, $CDCl_3$) δ 7.48–7.34 (m, 1H), 7.26–7.15 (m, 3H), 7.12–7.00 (m, 2H), 6.96 (d, J = 7.5 Hz, 1H), 6.67 (d, J = 7.9 Hz, 1H), 6.35 (s, 1H), 5.39 (s, 1H), 5.07 (t, J = 16.8 Hz, 1H), 4.86 (dd, J = 16.5, 8.6 Hz, 1H), 4.70–4.52 (m, 1H), 4.10 (s, 1H), 2.04 (s, 3H), 1.47 (s, 3H), 1.09 (s, 3H). ^{13}C NMR (100 MHz, $CDCl_3$) δ 189.05, 174.38, 170.51, 167.98, 143.52, 139.85, 133.03, 132.56, 130.03, 129.97, 129.80, 129.13, 128.10, 127.35, 125.92, 122.72, 122.04, 121.43, 111.81, 109.91, 104.49, 73.54, 71.06, 57.56, 55.48, 49.63, 45.89, 41.77, 37.98, 36.78, 36.72, 36.66, 34.36, 33.68, 32.45, 30.28, 27.62, 21.41, 20.07, 19.37, 14.70. HRMS (ESI): m/z calcd for $C_{39}H_{40}ClN_3NaO_4$ $(M + Na)^+$, 672.2605; found, 672.2600.

2.3.8. Compound **4h**

White solid, yield: 69%, m. p. 227.1–228.9 °C. ^{1}H NMR (400 MHz, $CDCl_3$) δ 7.33–7.20 (m, 3H), 7.19–6.97 (m, 3H), 6.92 (d, J = 7.4 Hz, 1H), 6.82 (dd, J = 25.3, 7.9 Hz, 1H), 6.40 (s, 1H), 5.38 (d, J = 4.2 Hz, 1H), 4.96 (dd, J = 27.2, 15.7 Hz, 1H), 4.80 (dd, J = 23.7, 15.7 Hz, 1H), 4.60 (dt, J = 10.7, 5.6 Hz, 1H), 4.04 (s, 1H), 2.04 (s, 3H), 1.45 (s, 3H), 1.09 (s, 3H). ^{13}C NMR (100 MHz, $CDCl_3$) δ 190.32, 189.07, 174.22, 171.56, 170.52, 168.42, 168.07, 144.00, 143.45, 140.25, 139.84, 129.98, 129.85, 129.74, 125.82, 124.96, 124.70, 124.66, 124.19, 123.64, 123.18, 122.55, 122.47, 122.32, 122.15, 122.07, 121.44, 121.05, 115.94, 115.73, 115.56, 115.34, 112.07, 111.86, 109.95, 109.64, 104.42, 102.78, 99.99, 73.54, 71.11, 57.55, 56.95, 55.26, 49.62, 45.84, 45.56, 37.98, 36.78, 36.71, 36.66, 34.35, 34.06, 33.59, 32.49, 32.43, 30.33, 30.27, 27.62, 21.40, 20.07, 19.39, 19.36, 14.84, 14.66. HRMS (ESI): m/z calcd for $C_{39}H_{40}FN_3NaO_4$ $(M + Na)^+$, 656.2901; found, 656.2902.

2.3.9. Compound **4i**

White solid, yield: 65%, m. p. 263.9–265.3 °C. ^{1}H NMR (400 MHz, $CDCl_3$) δ 7.29 (dd, J = 13.8, 5.8 Hz, 1H), 7.23 (t, J = 7.6 Hz, 1H), 6.76 (d, J = 7.9 Hz, 1H), 6.18 (m, 1H), 5.39 (d, J = 4.4 Hz, 1H), 5.06–4.89 (m, 2H), 4.70–4.54 (m, 1H), 4.01 (s, 1H), 2.04 (s, 3H), 1.45 (s, 3H), 1.09 (s, 3H). ^{13}C NMR (100 MHz, $CDCl_3$) δ 189.00, 173.52, 170.50, 167.93, 167.87, 162.72, 162.65, 160.25, 160.17, 143.06, 139.81, 130.37, 130.27, 129.80, 125.82, 122.50, 122.02, 121.47, 112.03, 111.87, 111.79, 110.82, 110.66, 109.12, 104.42, 73.55, 71.06, 71.02, 57.53, 55.09, 49.62, 45.84, 37.98, 36.78, 36.65, 34.35, 33.61, 32.43, 32.25, 30.27, 27.63, 21.40, 20.07, 19.35, 14.67. HRMS (ESI): m/z calcd for $C_{39}H_{39}F_2N_3$ NaO_4 $(M + Na)^+$, 674.2806; found, 674.2804.

2.3.10. Compound **4j**

White solid, yield: 64%, m. p. 216.6–218.5 °C. ^{1}H NMR (400 MHz, $CDCl_3$) δ 7.72 (d, J = 7.4 Hz, 1H), 7.40 (dt, J = 14.9, 7.3 Hz, 2H), 7.20 (t, J = 7.7 Hz, 1H), 7.06 (t, J = 7.7 Hz, 2H), 6.99 (d, J = 7.4 Hz, 1H), 6.57 (s, 1H), 6.52 (d, J = 7.8 Hz, 1H), 5.38 (d, J = 4.8 Hz, 1H), 5.26 (d, J = 17.3 Hz, 1H), 4.89 (d, J = 17.2 Hz, 1H), 4.70–4.54 (m, 1H), 4.15 (s, 1H), 2.04 (s, 3H), 1.49 (s, 3H), 1.10 (s, 3H). ^{13}C NMR (100 MHz, $CDCl_3$) δ 189.03, 174.59, 170.51, 168.12, 143.34, 139.86, 133.57, 132.49, 129.82, 128.02, 127.67, 126.61, 126.50, 126.45, 126.03, 125.67, 122.89, 122.04, 121.41, 111.70, 109.72, 104.57, 73.54, 71.12, 57.58, 55.57, 49.63, 45.91, 40.60, 37.98, 36.78, 36.66, 34.35, 33.68, 32.46, 30.27, 27.62, 26.92, 21.40, 20.08, 19.37, 14.71. HRMS (ESI): m/z calcd for $C_{40}H_{41}$ $F_3N_3O_4$ $(M + H)^+$, 684.3049; found, 684.3044.

2.4. Cell culturing

Human cancer cell lines were maintained in minimal essential medium supplemented with 10% fetal bovine serum (FBS) and 1% penicillin–streptomycin in a humidified atmosphere of 5% CO_2

and 95% air at 37 °C. Cancer cells were maintained in RPMI1640 medium. All cell lines were purchased from the China Center for Type Culture Collection (CCTCC, Shanghai, China). For pharmacological investigations, 10 mM stock solutions of the tested compounds were prepared with dimethyl sulfoxide (DMSO). The highest DMSO concentration of the medium (0.1%) did not have any substantial effect on the determined cellular functions.

2.5. Cytotoxic activity assays

Exponentially growing cells were seeded into 96-well plates at a concentration of 5×10^3 cells per well. After 24 h incubation at 37 °C, the culture medium was removed and replaced with fresh medium containing the candidate compounds in different concentrations. The cells were incubated for another 72 h. Then, 20 μL of MTT (3-(4, 5-dimethylthiazol-2-yl)-2, 5-diphenyltetrazolium bromide) solution (5 mg/mL) was added to all wells and incubated for 4 h at 37 °C. Discarded the suspension and added 150 μL of dimethyl sulfoxide (DMSO) to each well and shook the plates to dissolve the dark blue crystals (formazan); the absorbance was measured using a microplate reader at a wavelength of 490 nm. Each concentration was analyzed in triplicate and the experiment was repeated three times. The average 50% inhibitory concentration (IC_{50}) was determined from the dose-response curves according to the inhibition ratio for each concentration.

2.6. Analysis of cellular apoptosis

MGC-803 cells were plated in 6-well plates (5.0×10^6 cells/mL) and incubated at 37 °C for 24 or 48 h. Exponentially growing cells were then incubated for 24 or 48 h with complete medium (blank) or with the compound **4i**. Cells were then harvested and the Annexin-V-FITC/PI apoptosis kit (Biovision) was used according to the manufacturer's instructions to detect apoptotic cells. Ten thousand events were collected for each sample and analyzed by Accuri C6 flowcytometer.

2.7. Flow cytometric analysis of cell cycle distribution

For flow cytometric analysis of DNA content, 5.0×10^6 MGC-803 cells in exponential growth were treated with different concentrations of the test compound **4i** for 24 or 48 h. After an incubation period, the cells were collected, centrifuged and fixed with ice-cold ethanol (70%). The cells were then treated with buffer containing RNAse A and 0.1% Triton X-100 and then stained with PI. Samples were analyzed on Accuri C6 flow cytometer (Becton, Dickinson). Data obtained from the flow cytometer was analyzed using the FlowJo software (Tree Star, Inc., Ashland, OR, USA).

3. Results and discussion

3.1. Chemistry

The protocol for the synthesis of steroidal pyran–oxindole hybrids **4a–j** was straightforward using DBU-catalyzed cascade Aldol/cyclization process as the key step (Scheme 1). The intermediate **3** was prepared in high yield via Aldol condensation of 3β-acetyl dehydroepiandrosterone **2** with malononitrile in ethanol catalyzed by ammonium acetate following our previously reported methods [4,6]. In the presence of base, compounds **4a–j** were efficiently synthesized via the cascade Aldol/cyclization process of compound **3** and substituted isatins. Besides, we also investigated the effects of bases (Et_3N, DMAP, imidazole, pyridine, piperidine, $NaHCO_3$ and Na_2CO_3), solvents (toluene, DCM, EtOAc and MeOH) and the molar ratio toward the reaction between compound **3** and substituted isatins at room temperature, revealing that the optimized reaction condition was **3** (1.0 mmol), substituted isatin (1.0 mmol) and DBU (2.0 mmol) in EtOH (10 mL).

All the synthesized compounds were characterized by ^1H, ^{13}C NMR and high resolution mass spectra as described for compound **4i** (Fig. 3). In the ^1H NMR spectrum of compound **4i**, the signals of protons attached to CH_3CO-, C-19 and C-18 appeared at 2.04, 1.45 and 1.09 ppm respectively as sharp singlets. The signal of H-6 appeared at 5.38 ppm as a doublet ($J = 4.4$ Hz). The multiplet at 4.58–4.62 ppm was assigned to the 3α-H of steroid A-ring. The benzyl protons showed their peaks at 4.89–5.06 ppm as a multiplet (two protons). A broad peak that appeared at 6.14–6.21 ppm was assigned to the N–H proton due to the fact that there was no any correlation in the HSQC spectrum. The aromatic hydrogens appeared as doublets and multiplets at 6.75–7.32 ppm. Interestingly enough, the signal of H-16 appeared at 4.01 ppm as a sharp singlet and no coupling with protons attached to C-15 was observed although it was adjacent to a secondary carbon (C-15) as indicated in DEPT135, H–H COSY and HMBC spectra. This was probably attributed to the special space orientation between the H-16 and H-15 and there was no interaction between the H-16 and other protons as indicated in NOE spectrum. From the HSQC spectrum together with ^1H and ^{13}C NMR spectra, some direct C–H correlations were observed, confirming that the signals of the benzyl carbon, C-3, C-16, CH_3CO-, C-18 and C-19 appeared at 32.43, 73.55, 55.09, 21.40, 14.67 and 19.35 ppm, respectively. From the HMBC spectrum, we clearly found that both the N–H and H-16 had HMBC correlation with a quaternary carbon atom (indicated in

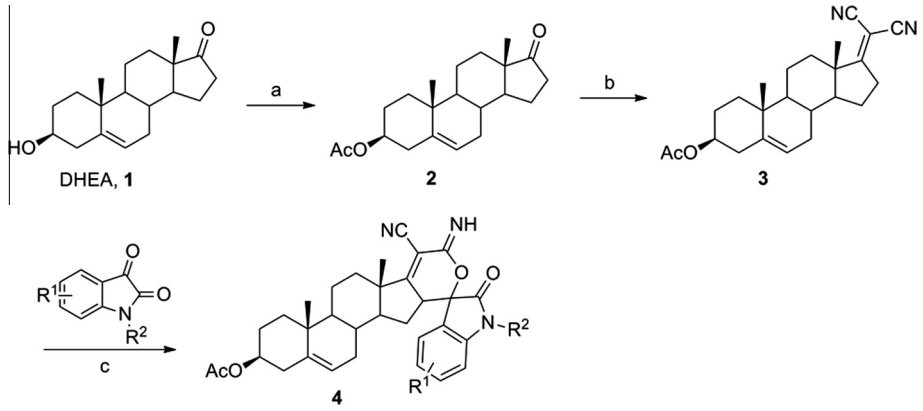

Scheme 1. Synthesis of steroidal pyran–oxindole hybrids **4a–j**. Reagents and conditions: (a) $(Ac)_2O$, DMAP, Et_3N, DCM, r.t; (b) malononitrile, NH_4OAc, EtOH, reflux; (c) DBU, EtOH, r.t.

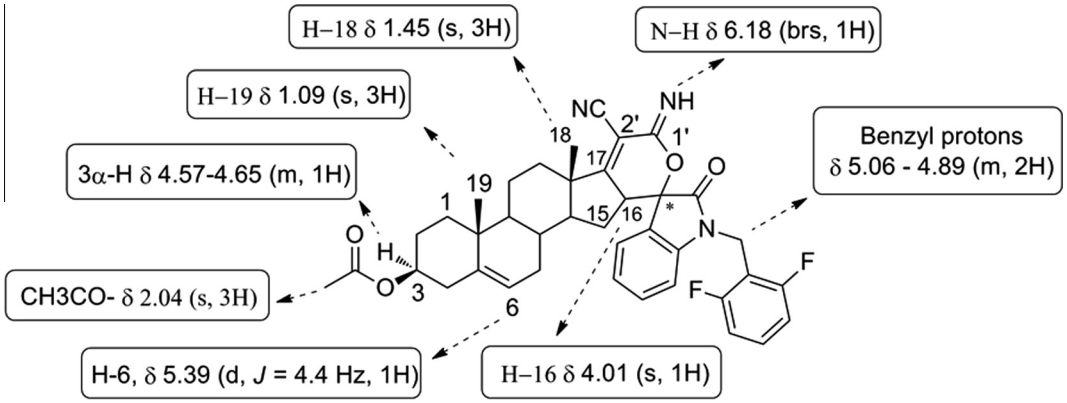

Fig. 3. Selected ^{1}H NMR chemical shifts of compound **4i.**

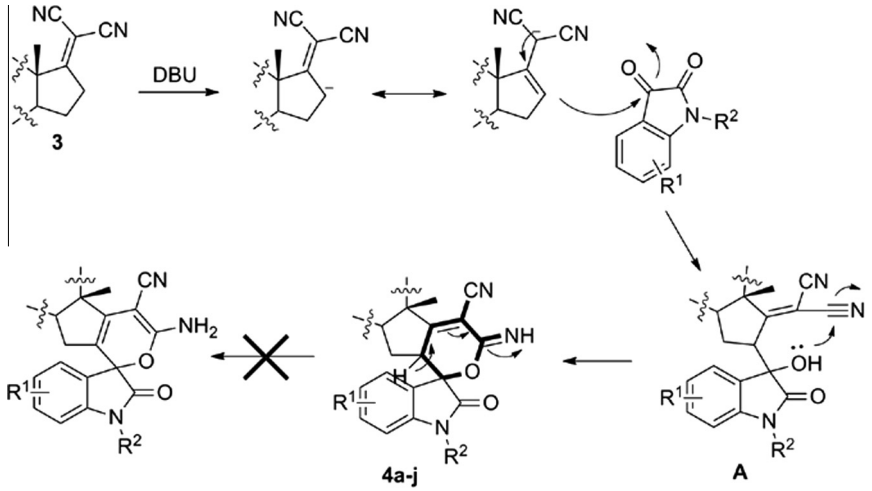

Scheme 2. Proposed reaction mechanism for the synthesis of steroidal pyran–oxindole hybrids **4a–j.**

DEPT135 spectrum) with its signal appearing at 71.06 ppm, proving that this carbon atom was the spiro carbon that linked the pyran and oxindole motif. A carbon atom whose signal appeared at 189.00 ppm had HMBC correlations with the N–H, H-15 and H-18, a phenomenon that in turn confirmed the chemical shift of C-17. Besides, the N–H proton had HMBC correlations with C-1′ (167.93 ppm) and C-2′ (104.42 ppm). The downfield chemical shift of C-17 and relatively upfield chemical shift of C-2′ were probably due to the inductive effects of the electron-withdrawing cyano group and 2-imino ester group attached to C-2′. The presence of a molecular ion peak at m/z = 674.2804 ($[M + Na]^+$) in the mass spectrum (calcd. 674.2806) further confirmed the structure of compound **4i**. For all the spectra of compound **4i**, please refer to the supporting information.

A possible mechanism for the formation of compounds **4a–j** was proposed in Scheme 2. In the presence of base, the first step

Table 1
Preliminary *in vitro* cytotoxic activities of steroidal pyran–oxindole hybrids against four human cancer cell lines.

Compounds	R^1	R^2	IC_{50} (μM)[a]			
			T24	SMMC-7721	MCF-7	MGC-803
4a	4-Br	H	49.00 ± 1.69	>128	24.12 ± 1.38	108.51 ± 2.04
4b	4-Cl	H	52.89 ± 1.72	80.53 ± 1.91	14.78 ± 1.20	14.45 ± 1.16
4c	H	Benzyl	>128	>128	57.52 ± 1.76	30.95 ± 1.49
4d	H	2′-Methylbenzyl	>128	>128	113.46 ± 2.01	40.17 ± 1.60
4e	H	3′-Methylbenzyl	>128	>128	69.14 ± 1.84	82.30 ± 1.92
4f	H	4′-Methylbenzyl	4.43 ± 0.86	117.87 ± 2.07	66.37 ± 1.07	89.88 ± 1.95
4 g	H	2′-Chlorobenzyl	>128	64.35 ± 1.81	46.31 ± 1.67	57.74 ± 1.76
4 h	H	2′-Fluorobenzyl	10.84 ± 1.04	30.84 ± 1.49	17.42 ± 1.24	10.05 ± 0.56
4i	H	2′, 6′-Difluorobenzyl	32.52 ± 1.51	>128	12.31 ± 0.98	8.45 ± 0.93
4j	H	3′-Trifluoromethylbenzyl	49.46 ± 1.69	>128	56.21 ± 0.81	>128
5-Fu	–	–	7.14 ± 0.85	4.29 ± 0.63	10.53 ± 1.56	9.13 ± 0.96

[a] Inhibitory activity was assayed by exposure for 72 h to substances and expressed as concentration required to inhibit tumor cell proliferation by 50% (IC_{50}). Data are presented as the means ± SDs of three independent experiments.

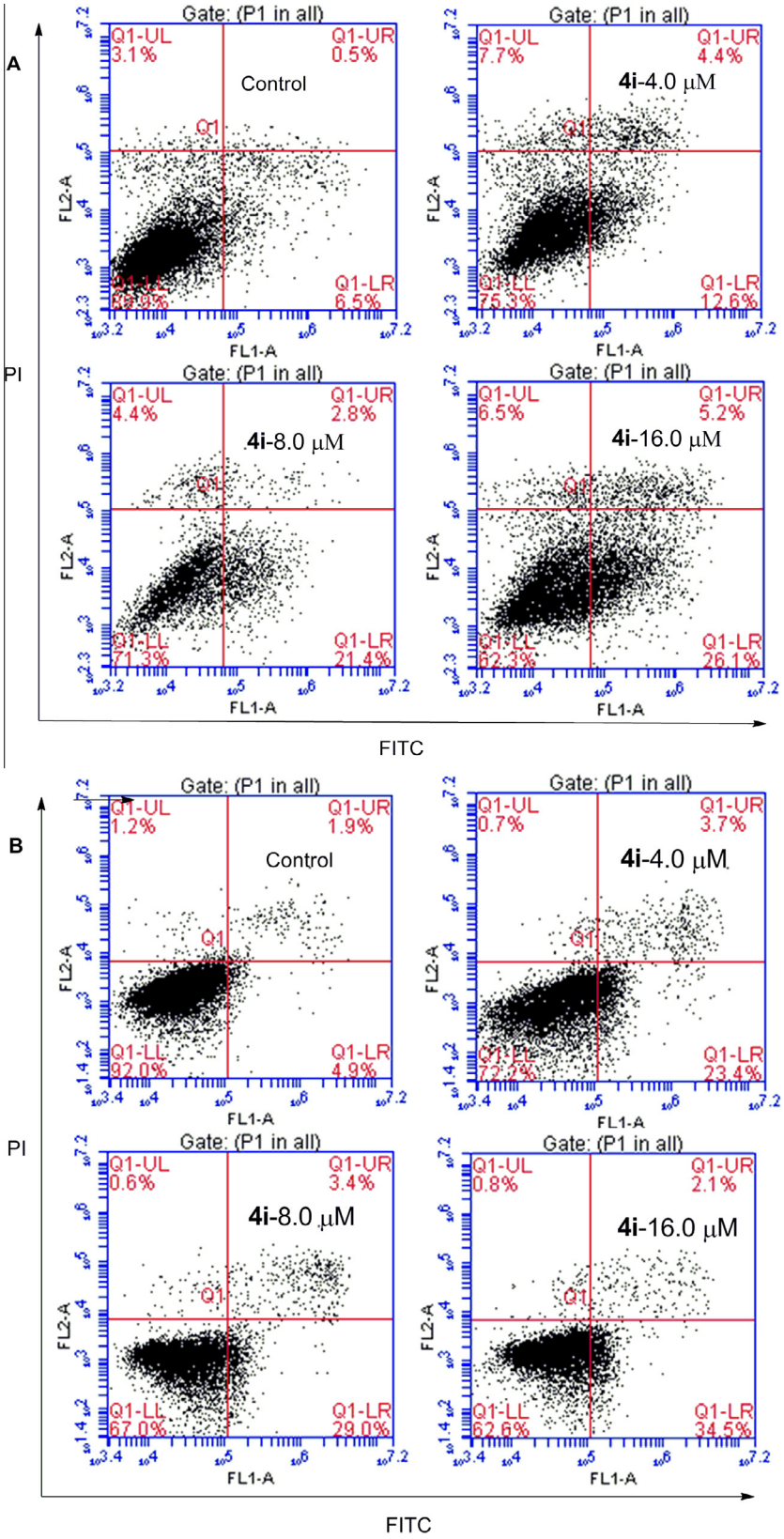

Fig. 4. Apoptosis effect on human MGC-803 cell line induced by compound **4i**. Apoptotic cells were detected with Annexin V-FITC/PI double staining after incubation with compound **4i** (0, 4.0, 8.0, 16.0 μM) for 24 h or 48 h. (A) Incubated for 24 h; (B) Incubated for 48 h. The lower left quadrants represent live cells, the lower right quadrants are for early/primary apoptotic cells, upper right quadrants are for late/secondary apoptotic cells, while the upper left quadrants represent cells damaged during the procedure. The experiments were performed three times, and a representative experiment is shown.

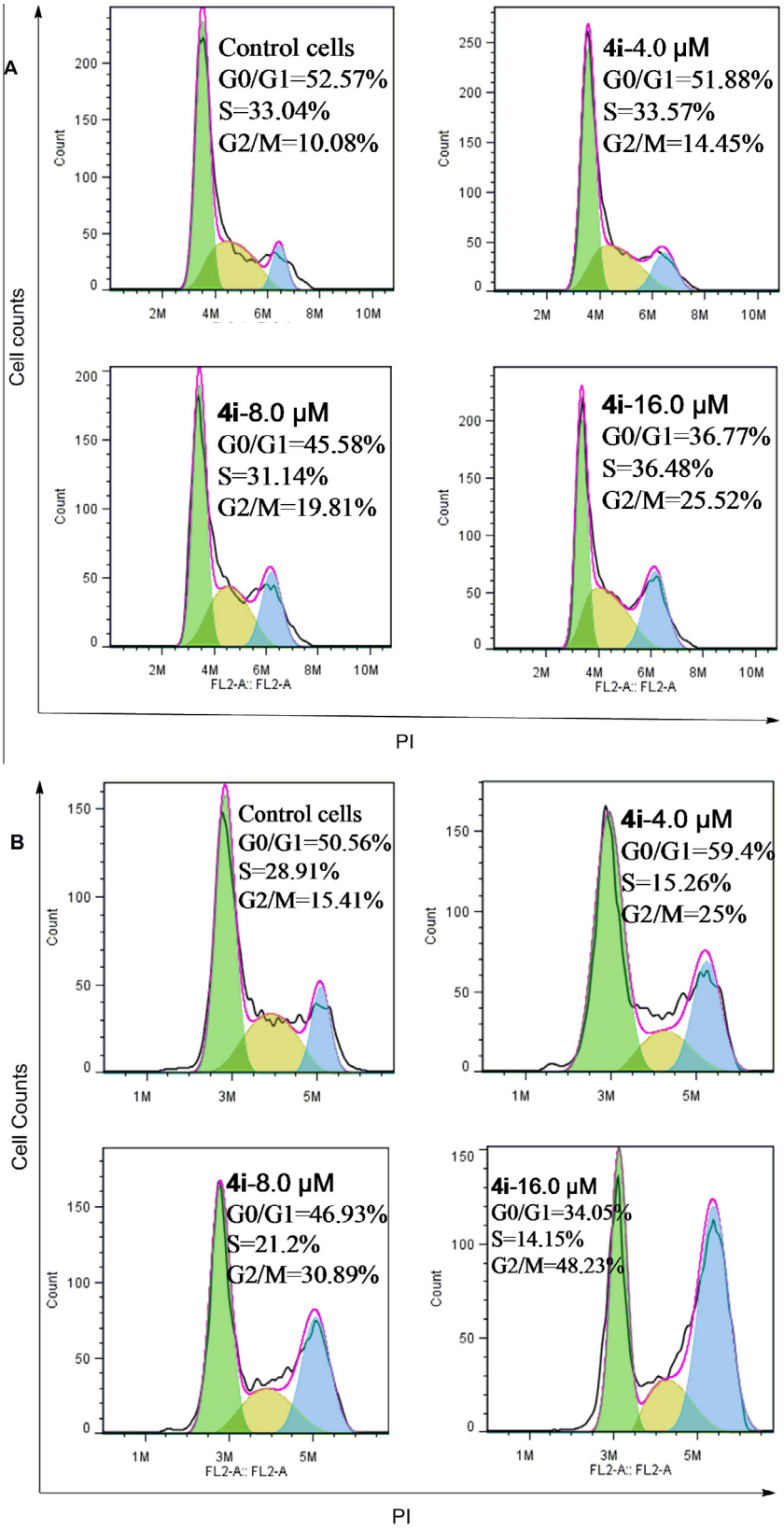

Fig. 5. Effect of compound **4i** on the cell cycle distribution of MGC-803 cells. Cells were treated with different concentrations (0, 4.0, 8.0, 16.0 μM) for 24 h or 48 h. Then the cells were fixed and stained with PI to analyze DNA content by flow cytometry. (A) Incubated for 24 h; (B) Incubated for 48 h. The experiments were performed three times, and a representative experiment is shown.

involved facile deprotonation of vinyl malononitrile (**3**) to furnish a nucleophile that attacked the isatin to form an aldol adduct (**A**) followed by the intramolecular cyclization in a tandem procedure, yielding the title compounds **4a–j**. Different from the findings reported by Thelagathoti Hari Babu and co-authors [26], further isomerization of compounds **4a–j** was not observed probably due to the relatively mild acidity of H-16. Functionalized steroidal pyran–oxindole hybrids were synthesized through the vinylogous aldol reaction of vinyl malononitrile with various isatin derivatives, involving tandem construction of C–C and C–O bonds and two continuous chiral centers (one of them was the quaternary carbon). The spiro-oxindole framework occupies a special place in heterocyclic chemistry because of the presence of this framework in a number of natural products, such as surugatoxin, horsfiline, etc. Aza-spiro derivatives are well known [27], but the preparation of the corresponding oxa-analogues has evolved at a relatively slow pace [28]. To the best of our knowledge, it is the first time to report the synthesis of functionalized steroidal oxa spiro-oxindoles.

3.2. Biological evaluation

3.2.1. Cytotoxic activities

The IC_{50} values (concentrations that are required to inhibit tumor cell proliferation by 50%) for the synthesized compounds against four human cancer cell lines including human bladder cancer cell line (T24), human liver cancer cell line (SMMC-7721), human breast cancer cell line (MCF-7) and human gastric cancer cell line (MGC-803), were determined using the MTT assay. The well-known anticancer drug 5-fluorouracil was also evaluated in parallel as a positive control and the results were listed in Table 1.

The structure–activity relationships (SARs) were probed through altering substituents in the oxindole and *N*-benzyl moieties. As shown in Table 1, most of the compounds showed moderate cytotoxic activities against four human cancer cell lines, and a relatively good selectivity was observed, compounds **4a–j** were generally found to be more active against MCF-7 and MGC-803 cells. It is also clear that substituents on the oxindole and *N*-benzyl moieties had remarkable effect on their cytotoxicity. Specifically, compound **4a** showed moderate inhibitory effect against MCF-7 cells (IC_{50} = 24.12 ± 1.38 μM), but was inactive to T24, SMMC-7721 and MGC-803 cells. Similarly, compound **4b** displayed weak inhibition against T24 and SMMC-7721 cells (IC_{50} > 52 μM), but showed moderate inhibition against MCF-7 and MGC-803 cells with the IC_{50} values ranging from 14.15 to 24.12 μM. For MGC-803 cells, compound **4b** was about 7–8 times more potent than compound **4a** with the IC50 values of 14.45 ± 1.16 and 108.51 ± 2.04 μM, respectively. For T24 cells, compounds **4a–j** showed distinguishing inhibitory effect, among them, compound **4f** with 4′-methyl substituent on the phenyl group exhibited excellent cytotoxicity (IC_{50} = 4.43 ± 0.86 μM) and was more potent than 5-Fu (IC_{50} = 7.14 ± 0.85 μM). By contrast, compounds **4c–e** were found to be inactive to T24 cells (IC_{50} > 128 μM), showing that the position of substituent had a remarkable effect on the cytotoxicity. In addition, compound **4g** with 2′-chloro substituent on the phenyl group also showed no activity as compound **4d** did. While compound **4h** with 2′-fluoro substituent showed significantly enhanced cytotoxic activity (IC_{50} = 10.84 ± 1.04 μM) compared with compound **4g**. Furthermore, when an additional fluoro atom (**4i**) or a trifluoromethyl group (**4j**) was introduced, the activity was decreased to varying degrees. For SMMC-7721 cells, all the compounds showed weak to moderate inhibition and were less potent than 5-Fu. Compound **4f** with the most excellent activity against T24 cells had weak inhibitory effect against MCF-7 and MGC-803 cells with the IC_{50} values of 66.37 ± 1.07 and 89.88 ± 1.95 μM, respectively. Fluorinated compounds **4h–i** displayed excellent cytotoxicity activities against MCF-7 and MGC-803 cells with the IC_{50} values ranging from 8.45 to 17.42 μM. Particularly, compound **4i** was the most cytotoxic one with the IC_{50} value of 8.45 ± 0.93 μM and potent than 5-Fu. On the basis of those discussed above, we can conclude that the electronic effect and positions of substituents on the oxindole and *N*-benzyl group has a remarkable but different effect on the cytotoxicity against all the cancel cells tested.

3.2.2. Apoptosis assay

Due to the good cytotoxic activity against some of tested human cancer cell lines, compound **4i** was chosen to be further investigated regarding its mechanism of action. In order to better characterize the mode of cell death induced by compound **4i**, we performed a biparametric cytofluorimetric analysis using propidium iodide (PI) and Annexin V-FITC in MGC-803 cells. After treatment with compound **4i** for 24 or 48 h at different concentrations (0, 4.0, 8.0, 16.0 μM), MGC-803 cells were labeled with two dyes, and the resulting red (PI) and green (FITC) fluorescence was monitored by flow cytometry. It can be observed from Fig. 4 that compound **4i** caused the early apoptosis. Specifically, after treatment for 24 h, when the concentration was 4.0 μM, the early apoptosis rate was 12.6%, and for the high concentration group (16.0 μM), the early and late apoptosis rates were 26.1% and 5.2%, respectively (6.5% and 0.5% for the control group) (Fig. 4A). Similarly, the early rate for the high concentration group (16.0 μM) was 34.5% after treatment for 48 h. The results showed that compound **4i** markedly increased the cellular apoptosis in a concentration- and time-dependent manner.

3.2.3. Cell cycle analysis

To better understand the cytotoxic activity of compound **4i**, a cell-cycle assay was performed by treating MGC-803 cells at different concentrations of compound **4i** (0, 4.0, 8.0, 16.0 μM). After treatment MGC-803 cells with compound **4i** for 24 h, the percentage of cells in G2/M phase at different concentrations were 10.08%, 14.45%, 19.81% and 25.52%, respectively (Fig. 5A), whereas when treatment for 48 h, the percentage of cells in G2/M phase were 15.41%, 25.00%, 30.89% and 48.23%, respectively (Fig. 5B). The results suggested that **4i** caused an obvious G2/M arrest in a concentration- and time-dependent manner with a concomitant decrease in terms of the number of cells in other phases of the cell cycle.

4. Conclusion

In summary, we first reported the efficient one-pot synthesis of novel steroidal pyran–oxindole hybrids under mild conditions through the vinylogous Aldol reaction of vinyl malononitrile with various isatin derivatives. This procedure involved cascade construction of C–C and C–O bonds. Some of these compounds displayed weak to moderate cytotoxicity against T24, SMMC-7721, MCF-7 and MGC-803 cells and were sensitive to MCF-7 and MGC-803 cells. Compounds **4f** and **4i** were more potent than 5-Fu against T24 and MGC-803 cells with the IC_{50} values of 4.43 and 8.45 μM respectively. Further mechanism studies indicated that compound **4i** induced G2/M arrest and early apoptosis in a concentration- and time-dependent manner. Synthesis of more analogues, SAR studies and further mechanism investigations are under way and will be reported in due course.

Acknowledgment

This work was supported by the National Natural Science Foundation of China (No. 21372206).

Appendix A. Supplementary data

Supplementary data associated with this article can be found, in the online version, at http://dx.doi.org/10.1016/j.steroids.2014.05.022.

References

[1] Singh R, Panda G. An overview of synthetic approaches for heterocyclic steroids. Tetrahedron 2013;69:2853–84.
[2] Frank É, Schneider G. Synthesis of sex hormone-derived modified steroids possessing antiproliferative activity. J. Steroid Biochem. Mol. Biol. 2013;137:301–15.
[3] Salvador JA, Carvalho JF, Neves MA, Silvestre SM, Leitao AJ, Silva MM, Sa e Melo ML. Anticancer steroids: linking natural and semi-synthetic compounds. Nat. Prod. Rep. 2013;30:324–74.
[4] Yu B, Shi XJ, Ren JI, Sun XN, Qi PP, Fang Y, Ye XW, Wang MM, Wang JW, Zhang E, Yu DQ, Liu HM. Efficient construction of novel D-ring modified steroidal dienamides and their cytotoxic activities. Eur. J. Med. Chem. 2013;66:171–9.
[5] Yu B, Sun XN, Shi XJ, Qi PP, Fang Y, Zhang E, Yu DQ, Liu HM. Stereoselective synthesis of novel antiproliferative steroidal (*E*, *E*) dienamides through a cascade aldol/cyclization process. Steroids 2013;78:1134–40.
[6] Yu B, Zhang E, Sun XN, Ren JL, Fang Y, Zhang BL, Yu DQ, Liu HM. Facile synthesis of novel D-ring modified steroidal dienamides via rearrangement of 2*H*-pyrans. Steroids 2013;78:494–9.
[7] Piotrowski DW. Mineralocorticoid receptor antagonists for the treatment of hypertension and diabetic nephropathy. J. Med. Chem. 2012;55:7957–66.
[8] Purushottamachar P, Godbole AM, Gediya LK, Martin MS, Vasaitis TS, Kwegyir-Afful AK, Ramalingam S, Ates-Alagoz Z, Njar VCO. Systematic structure modifications of multitarget prostate cancer drug candidate galeterone to produce novel androgen receptor down-regulating agents as an approach to treatment of advanced prostate cancer. J. Med. Chem. 2013;56:4880–98.
[9] Yu B, Shi XJ, Zheng YF, Fang Y, Zhang E, Yu DQ, Liu HM. A novel [1,2,4] triazolo [1,5-a] pyrimidine-based phenyl-linked steroid dimer: Synthesis and its cytotoxic activity. Eur. J. Med. Chem. 2013;69:323–30.
[10] Galliford CV, Scheidt KA. Pyrrolidinyl–spirooxindole natural products as inspirations for the development of potential therapeutic agents. Angew. Chem. Int. Ed. 2007;46:8748–58.
[11] Singh GS, Desta ZY. Isatins as privileged molecules in design and synthesis of spiro-fused cyclic frameworks. Chem. Rev. 2012;112:6104–55.
[12] Ding K, Lu Y, Nikolovska-Coleska Z, Wang G, Qiu S, Shangary S, Gao W, Qin D, Stuckey J, Krajewski K, Roller PP, Wang S. Structure-based design of spiro-oxindoles as potent, specific small-molecule inhibitors of the MDM2−p53 interaction. J. Med. Chem. 2006;49:3432–5.
[13] Bhaskar G, Arun Y, Balachandran C, Saikumar C, Perumal PT. Synthesis of novel spirooxindole derivatives by one pot multicomponent reaction and their antimicrobial activity. Eur. J. Med. Chem. 2012;51:79–91.
[14] Kia Y, Osman H, Kumar RS, Murugaiyah V, Basiri A, Perumal S, Wahab HA, Bing CS. Synthesis and discovery of novel piperidone-grafted mono- and bis-spirooxindole-hexahydropyrrolizines as potent cholinesterase inhibitors. Biorg. Med. Chem. 2013;21:1696–707.
[15] kia Y, Osman H, Kumar RS, Murugaiyah V, Basiri A, Perumal S, Razak IA. A facile chemo-, regio- and stereoselective synthesis and cholinesterase inhibitory activity of spirooxindole-pyrrolizine-piperidine hybrids. Bioorg. Med. Chem. Lett. 2013;23:2979–83.
[16] Parthasarathy K, Praveen C, Balachandran C, Senthil Kumar P, Ignacimuthu S, Perumal PT. Cu(OTf) catalyzed three component reaction: Efficient synthesis of spiro[indoline-3,4'-pyrano[3,2-b] pyran derivatives and their anticancer potency towards A549 human lung cancer cell lines. Bioorg. Med. Chem. Lett. 2013;23:2708–13.
[17] Yu LF, Li YY, Su MB, Zhang M, Zhang W, Zhang LN, Pang T, Zhang RT, Liu B, Li JY, Li J, Nan FJ. Development of novel alkene oxindole derivatives as orally efficacious AMP-activated protein kinase activators. ACS Med. Chem. Lett. 2013;4:475–80.
[18] Rottmann M, McNamara C, Yeung BK, Lee MC, Zou B, Russell B, Seitz P, Plouffe DM, Dharia NV, Tan J, Cohen SB, Spencer KR, Gonzalez-Paez GE, Lakshminarayana SB, Goh A, Suwanarusk R, Jegla T, Schmitt EK, Beck HP, Brun R, Nosten F, Renia L, Dartois V, Keller TH, Fidock DA, Winzeler EA, Diagana TT. Spiroindolones, a potent compound class for the treatment of malaria. Science 2010;329:1175–80.
[19] Yu J, Shi F, Gong LZ. Brønsted-acid-catalyzed asymmetric multicomponent reactions for the facile synthesis of highly enantioenriched structurally diverse nitrogenous heterocycles. Acc. Chem. Res. 2011;44:1156–71.
[20] Bertamino A, Aquino C, Sala M, Simone ND, Mattia CA, Erra L, Musella S, Iannelli P, Carotenuto A, Grieco P, Novellino E, Campiglia P, Gomez-Monterrey I. Design and synthesis of spirotryprostatin-inspired diketopiperazine systems from prolyl spirooxoindolethiazolidine derivatives. Bioorg. Med. Chem. 2010;18:4328–37.
[21] Ding K, Lu Y, Nikolovska-Coleska Z, Qiu S, Ding Y, Gao W, Stuckey J, Krajewski K, Roller PP, Tomita Y, Parrish DA, Deschamps JR, Wang S. Structure-based design of potent non-peptide MDM2 inhibitors. J. Am. Chem. Soc. 2005;127:10130–1.
[22] Dickinson JM. Microbial pyran-2-ones and dihydropyran-2-ones. Nat. Prod. Rep. 1993;10:71–98.
[23] Kemnitzer W, Jiang S, Zhang H, Kasibhatla S, Crogan-Grundy C, Blais C, Attardo G, Denis R, Lamothe S, Gourdeau H, Tseng B, Drewe J, Cai SX. Discovery of 4-aryl-2-oxo-2*H*-chromenes as a new series of apoptosis inducers using a cell- and caspase-based high-throughput screening assay. Biorg. Med. Chem. Lett. 2008;18:5571–5.
[24] Kemnitzer W, Drewe J, Jiang S, Zhang H, Wang Y, Zhao J, Jia S, Herich J, Labreque D, Storer R, Meerovitch K, Bouffard D, Rej R, Denis R, Blais C, Lamothe S, Attardo G, Gourdeau H, Tseng B, Kasibhatla S, Cai SX. Discovery of 4-aryl-4*H*-chromenes as a new series of apoptosis inducers using a cell- and caspase-based high-throughput screening assay. 1. Structure−activity relationships of the 4-aryl group. J. Med. Chem. 2004;47:6299–310.
[25] Yu B, Shi XJ, Qi PP, Yu DQ, Liu HM. Design, synthesis and biological evaluation of novel steroidal spiro-oxindoles as potent antiproliferative agents. J. Steroid Biochem. Mol. Biol. 2014;141:121–34.
[26] Babu TH, Karthik K, Perumal PT. A Facile, one-pot synthesis of functionalized spiro-oxindoles via vinylogous aldol reaction of vinyl malononitriles with isatin derivatives in aqueous media. Synlett 2010;2010:1128–32.
[27] Liu Y, Wang H, Wan J. Recent advances in diversity oriented synthesis through isatin-based multicomponent reactions. Asian J. Org. Chem. 2013;2:374–86.
[28] Han YY, Chen WB, Han WY, Wu ZJ, Zhang XM, Yuan WC. Highly efficient and stereoselective construction of dispiro-[oxazolidine-2-thione] bisoxindoles and dispiro[imidazolidine-2-thione] bisoxindoles. Org. Lett. 2013;14:490–3.